Rotational microfluidic motor for on-chip microcentrifugation

Richie J. Shilton, Nick R. Glass, Peggy Chan, Leslie Y. Yeo, and James R. Friend[a)]
MicroNanophysics Research Laboratory, Monash University, Clayton, Victoria 3800, Australia and The Melbourne Centre for Nanofabrication, Clayton, Victoria 3800, Australia

(Received 1 May 2011; accepted 23 May 2011; published online 24 June 2011)

We report on the design of a surface acoustic wave (SAW) driven fluid-coupled micromotor which runs at high rotational velocities. A pair of opposing SAWs generated on a lithium niobate substrate are each obliquely passed into either side of a fluid drop to drive rotation of the fluid, and the thin circular disk set on the drop. Using water for the drop, a 5 mm diameter disk was driven with rotation speeds and start-up torques up to 2250 rpm and 60 nN m, respectively. Most importantly for lab-on-a-chip applications, radial accelerations of 172 m/s^2 was obtained, presenting possibilities for microcentrifugation, flow sequencing, assays, and cell culturing in truly microscale lab-on-a-chip devices. © *2011 American Institute of Physics*. [doi:10.1063/1.3600775]

Owing to the inadequacy of existing motor technology, small-scale actuators and motors are progressively becoming more important for the development of portable devices for a diverse number of applications.[1] For example, surgical tools,[2] actuators for biological analysis, cells,[3,4] and diagnostics[5,6] are a few of the many areas in which microscale actuation is required. Though there has been some progress, this has been limited by difficulties in attaining high-speed rotational motion.[7]

A variety of forces at the microscale have been employed to generate actuation at small scales, including electrostatic forces,[8] ultrasonically excited microbubbles,[3] piezoelectric ultrasonic resonance,[2] external magnets,[9] and capillary rotary action,[7] among others. Nevertheless, the motor designs arising from the use of such forces often require complex and precise designs, or are inadequate in either rotation speed or torque for most conceivable lab-on-a-chip applications.[10] Even if the motors can be adequately miniaturized, the required power supplies, amplifiers, transducers, magnets, and other ancillary equipment often cannot be scaled down.

To actuate our rotary micromotor, we generate an azimuthally rotating flow throughout a fluid drop via acoustic irradiation of geometrically tailored *surface acoustic waves* (SAWs). This coupled design, the large mass flow that may be induced by acoustic irradiation in comparison to other types of flow, and the large amount of power that may be transmitted using SAW, altogether makes it possible to drive the rotation of a thin disk at relatively high rotation speeds. The maximum speed of the disk is defined at a threshold at which its rotation becomes unstable and begins to precess.

SAWs, in general, have been shown to be a powerful means for driving fluid actuation.[11,12] Rapid and versatile actuation in the case of SAWs arises from the coupling between the fluid and the piezoelectric substrate in which the SAW is generated. Owing to the mismatch of sound velocities in the fluid and the substrate, the SAW radiates into a fluid along its propagation pathway and generates a pressure front in the fluid causing the bulk recirculation known as *acoustic streaming*—a surprisingly complex phenomenon that requires care in analysis and physical interpretation.[12] SAW *microcentrifugation*, in particular, has already been demonstrated for a variety of functions, including micromixing, particle concentration, and sorting.[13–16]

Two examples of a SAW-driven micromotor have previously been demonstrated in the literature; a sliding motor[10] and a rotational motor.[17] The rotors in these devices were supported by steel ball bearings placed on the substrate; dry friction contact is common in ultrasonic motors, of which SAW-driven motors are a fairly unique subset. Shigematsu's motors reported linear speeds over 1.5 m/s but required significant preloading[10] and exhibited rapid wear. To obtain rotational motion, the motor described by Zhang *et al.*[17] required a more complex motor design involving both supporting and freely moving steel ball bearings, which can be problematic when scaling down owing to wear and stiction. Furthermore, this motor only achieved a maximum of 180 rpm. By exploiting a fluid coupling layer, we demonstrate that it is possible to obtain rotational speeds over one order of magnitude larger than previously reported. The proposed motor design has no mechanically moving parts other than the rotor and requires no preload between the rotor and stator of the motor to enforce a frictional contact between them. There is no wear, nor is there a need for bearings, springs, and the like that are difficult to fabricate or are unreliable at small scales.

We now report on the design of a SAW driven fluid-coupled 5 mm rotary micromotor that can generate high-speed rotation of up to 2250 rpm that can be easily incorporated into microfluidics with modest power requirements suitable for a truly portable lab-on-a-chip device.

A typical SAW device used in microfluidics consists of a pair of interdigital transducers (IDTs) patterned onto a piezoelectric (lithium niobate) substrate, as shown in Fig. 1(a). The SAW energy is confined within a few wavelengths below the surface of the substrate until the SAW encounters the fluid, at which point, the energy transfers into the drop to constitute a very efficient mechanism for energy transport into the fluid. In this work, the IDTs are placed such that a Rayleigh wave will be induced along the surface. 128° Y-cut, X-propagating lithium niobate wafers were used as a substrate where 300 nm of gold with a 5 nm chromium adhesion layer was used for the IDTs. The IDTs consisted of 20 straight finger pairs with an aperture of approximately

a)Electronic mail: james.friend@monash.edu.

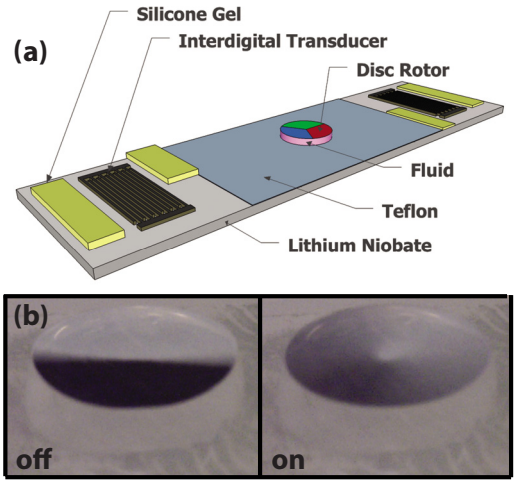

FIG. 1. (Color online) (a) Schematic of the isometric projection of the device (not to scale). To break the symmetry of the planar SAW wave into the fluid drop, opposite halves of the SAW generated at the IDTs from both sides of the device were absorbed with silicone gel as shown. The resulting bulk rotation of the fluid drop then caused the disk rotor placed on the fluid to spin. (b) The disk shown in static and rotating states (Video 1, enhanced online). [URL: http://dx.doi.org/10.1063/1.3600775.1]

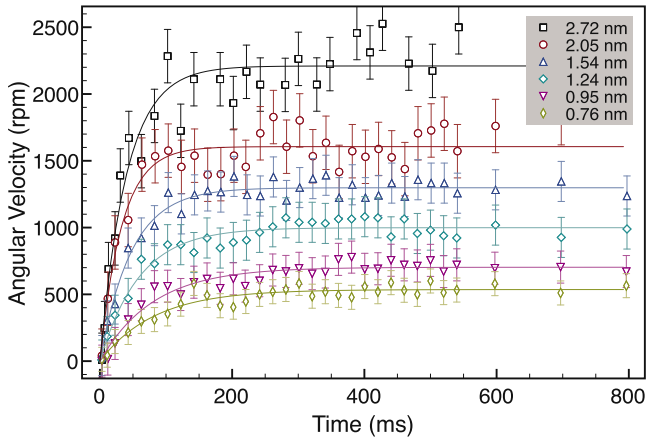

FIG. 2. (Color online) Rotation velocity (rpm) over time for a range of average SAW amplitudes for the disk. For each case, a 50 μl volume of water was used for the fluid coupling layer. The fitted curves are least-squares exponential fits commonly used for ultrasonic motor performance estimation as developed by Nakamura *et al.*; within the error in angular velocity that arises from extraction of the velocity data from high-speed video; the error between repeated runs is far smaller.

10 mm with a nominal resonant frequency of 20 MHz. Teflon was spun onto each device to form a potential well to hold the fluid drop. Disk rotors of 5 mm diameter were fabricated by punching them from a patterned 100 μm thick mylar sheet as seen in rotational motion in Fig. 1(b).

In a typical experiment, the rotor was carefully balanced on top of a small water drop of known volume. The mutually opposing SAW radiation propagating into the drop with a lateral offset with respect to the drop's center was chosen to generate acoustic radiation in the drop that is symmetric about its center. To this effect, half the SAWs generated from each IDT were absorbed using silicone blocks placed at either end of the substrate. A 20 MHz ac signal was connected to each IDT to generate the SAWs. We measured the transverse displacement amplitude of the SAW using a laser Doppler vibrometer. During experiments, videos were taken with a high speed camera (iSpeed, Olympus, Essex, U.K.), and angular displacements were measured from these image sequences, from which angular velocities and accelerations were calculated.

The SAW amplitude is a function of the input power applied across the pairs of IDTs. The rotational speeds were found to intensify linearly with an increase in the average surface displacement up to a maximum of up to 2250 rpm in this case. Over the range of surface displacements, the electrical input power applied to each IDT was between 0.1 and 1 W, although a substantial amount of this power is actually absorbed by the silicone dampers at either end of the trial device used for this study. The power actually used in propelling the fluid and rotating the disk is therefore a small fraction of this input power. As we increase the electrical input power beyond about 1 W, the average surface displacement surpasses ~3 nm and the disk rotation becomes unstable from the appearance of asymmetric flow in the drop. The disk rotates with precession at a reduced speed, and as the power is increased further this precession becomes more pronounced and the disk rotation decreases rapidly. The energy supplied to the fluid was insufficient to cause any liquid atomization of the fluid layer.[11] Evaporation was also negligible over the short timescales of each run. For extended use of such a motor, fluids other than water may be better suited to avoid fast evaporation of the fluid coupling layer.

The rotation spin-up of rotors in many piezoelectric motors is known to be a first-order dynamic response that may be modeled using an exponential curve-fit.[2,18] To determine the maximum torque exerted by the rotor, we fit a start-up curve to the rotation velocity-time data in Fig. 2 using the least-squares method as follows:

$$\omega(t) = \omega_{ss}(1 - e^{t/\tau}), \tag{1}$$

where $\omega(t)$ is the unloaded rotation speed, ω_{ss} is its steady-state value, t is the time, and τ is the characteristic time constant. If this model adequately represents the experimental data, as the rotor begins to spin, the torque exerted by the fluid is the maximum possible torque, and as the rotor accelerates to its maximum rotation speed—the *no-load speed*—we are able to completely define the performance behavior of the system with only these two values. As seen in Fig. 2, the first-order response model agrees well with the experimental results within the error of the measured values. Regardless of the amplitude of the SAW input, the rotor reaches its maximum rotational speed in under 200 ms. The angular velocity curves for the given surface displacements and the curve fits are shown in Fig. 2, from which it is possible to determine the maximum acceleration of the disk.[19] By measuring the mass of the disks, the maximum torque generated as a function of surface displacement can then be calculated from these values, as summarized in Fig. 3. Fourier analysis of the rotor velocity data in Fig. 2 suggests that the fluctuations in the velocity, particularly at high SAW amplitudes were due to random perturbations and not a periodic phenomenon.

The maximum torque increases substantially as the SAW amplitude is increased to around 2.5 nm. Beyond this displacement amplitude, however, the maximum torque drops rapidly. As discussed above, the decrease in the torque can be attributed to instabilities in the disk rotation at higher powers that lead to a small drop in the maximum rotational speed; we also notice precession of the disk's motion during rota-

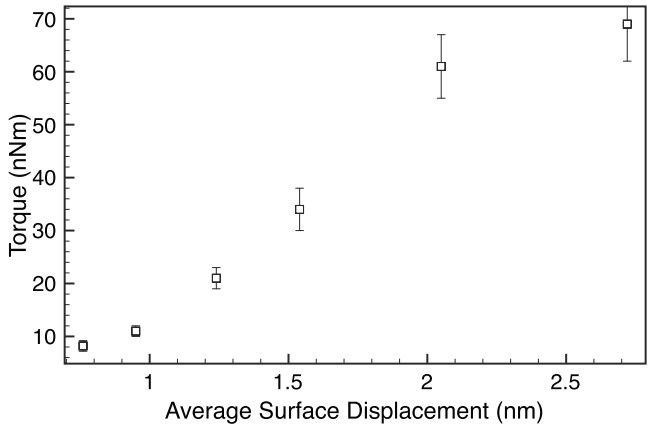

FIG. 3. Calculated maximum torque as a function of the average substrate SAW displacement for the disk with a 50 μl water coupling layer. The torque increases substantially until the disk begins to precess at around 2.5 nm surface displacement. The error bars appear from the error in measuring angular velocity as shown in the data taken and plotted in Fig. 2.

tion as the instability arises. The maximum torque that can be achieved at any SAW displacement amplitude with a 5 mm mylar disk with a 50 μL water coupling layer is 69 ± 7 nNm. This value is consistent or larger than other reported micromotor torque values while running at similar powers and at similar scales.[2,3]

A SAW driven fluid-coupled rotating micromotor has been demonstrated. The device consisted of a circular 5 mm disk rotor coupled with a fluid drop contained in a potential well placed asymmetrically in the propagation pathway of two counter-propagating SAWs. The motor was observed to spin up to its maximum speed in under 200 ms and the rotation speeds were found to vary linearly with the amplitude of the SAW, which can be controlled by varying the input power. The maximum torque that can be generated was found to be over 60 nN m, rotating at approximately 2250 rpm. The limit in performance of this motor in the current configuration is the appearance of radially asymmetric flow leading to precession and radial displacement of the rotor. Providing a simple, miniaturized method for driving efficient and fast rotary motion, the main attraction of the technique is its ability to be incorporated into lab-on-a-chip devices. Unlike other motors which require large ancillary equipment to provide the external forcing, true integrated functionality is possible with the SAW rotary micromotor given its simplicity and low power requirements.

The authors gratefully appreciate funding of this research from a CSIRO Flagship Project Grant on Sensor Systems for Analysis of Aquatic Environments. J.R.F. wishes to dedicate this work to the memory of his former student, Dr. Natsuki Yoshizumi, who passed away suddenly on 1 December 2010 from an industrial accident while conducting acoustics research near Tokyo. L.Y.Y. is funded through an Australian Research Fellowship granted by the Australian Research Council under Discovery Project Grant No. DP0985266. Authors Nick Glass and Richie Shilton contributed equally to this work.

[1]B. Watson, J. Friend, and L. Yeo, Sens. Actuators, A **152**, 219 (2009).
[2]B. Watson, J. Friend, and L. Yeo, J. Micromech. Microeng. **20**, 115018 (2010).
[3]J. Kao, X. Wang, J. Warren, J. Xu, and D. Attinger, J. Micromech. Microeng. **17**, 2454 (2007).
[4]P. Marmottant and S. Hilgenfeldt, Proc. Natl. Acad. Sci. U.S.A. **101**, 9523 (2004).
[5]C. Wang and G. Lee, Biosens. Bioelectron. **21**, 419 (2005).
[6]M. Madou, J. Zoval, G. Jia, H. Kido, J. Kim, and N. Kim, Annu. Rev. Biomed. Eng. **8**, 601 (2006).
[7]A. Takei, K. Matsumoto, and I. Shomoyama, Lab Chip **10**, 1781 (2010).
[8]Y.-C. Tai and R. S. Muller, Sens. Actuators, A **21**, 180 (1990).
[9]Y. Tian, Y. Zhang, J. Ku, Y. He, B. Xu, Q. Chen, H. Xia, and H. Sun, Lab Chip **10**, 2902 (2010).
[10]T. Shigematsu, M. Kurosawa, and K. Asai, IEEE Trans. Ultrason. Ferroelectr. Freq. Control **50**, 376 (2003).
[11]L. Y. Yeo and J. R. Friend, Biomicrofluidics **3**, 012002 (2009).
[12]J. R. Friend and L. Y. Yeo, Rev. Mod. Phys. **83**, 647 (2011).
[13]H. Li, J. Friend, and L. Yeo, Biomed. Microdevices **9**, 647 (2007).
[14]R. Shilton, M. Tan, L. Yeo, and J. Friend, J. Appl. Phys. **104**, 014910 (2008).
[15]P. Rogers, J. Friend, and L. Yeo, Lab Chip **10**, 2979 (2010).
[16]Y. Bourquin, J. Reboud, R. Wilson, and J. Cooper, Lab Chip **10**, 1898 (2010).
[17]G.-M. Zhang, L. Cheng, S. Zhang, J. Yu, and X. Shui, Electron. Lett. **36**, 1437 (2000).
[18]J. Friend, Y. Gouda, K. Nakamura, and S. Ueha, IEEE Trans. Ultrason. Ferroelectr. Freq. Control **53**, 1160 (2006).
[19]K. Nakamura, M. Kurosawa, H. Kurebayashi, and S. Ueha, IEEE Trans. Ultrason. Ferroelectr. Freq. Control **38**, 481 (2002).